Experimental Observations of Soliton Wave Trains in Electron Beams

Y. C. Mo, R. A. Kishek, D. Feldman, I. Haber, B. Beaudoin, P. G. O'Shea, and J. C. T. Thangaraj*

Institute for Research in Electronics and Applied Physics, University of Maryland, College Park, Maryland 20742, USA

(Received 7 November 2012; published 20 February 2013)

The first experimental observation of a Korteweg–de Vries-type soliton wave train in intense electron beams is reported. A narrow, large-amplitude perturbation on a long-pulse beam is observed to steepen and spawn a soliton wave train. The pulse width and amplitude of each peak remain unchanged over a long propagation distance, and the amplitude is inversely proportional to the square of the width. Two such pulses are seen to pass through each other, emerging from the collision unchanged. The experimental results are reproduced by particle-in-cell simulations.

DOI: 10.1103/PhysRevLett.110.084802 PACS numbers: 29.27.Bd, 29.27.Fh, 52.35.Sb

Solitons are localized persistent waves that behave like particles, preserving their properties (shape, velocity, etc.) over long distances and through interactions and collisions with other solitons. They are of interest to many disciplines such as condensed matter physics, plasma physics, particle physics, optics, biology, and medicine. First observed in water waves by Russell in 1834 [1], the unchanged propagating wave was named a "solitary wave" and was later described by the Korteweg–de Vries (KdV) equation in 1898. In 1965, Zabusky and Kruskal solved the KdV equation numerically and observed that solitary waves behave like stable particles [2], naming it a "soliton" afterward. In 1970, Ikezi, Taylor, and Baker observed ion-acoustic solitons in plasma experimentally [3]. Intense charge particle beams are known to have collective effects similar to plasmas [4], such as the ability to support waves. However, the beam system, a bounded non-neutral plasma, can behave in ways that differ fundamentally from an unbounded plasma. Since the 1980s, solitons have been predicted in charged particle beams, both in theory and in simulations [5–11]. Experiments on proton beams exhibited longitudinal single-soliton hole structures [12,13].

High brightness electron beams have wide applications in accelerator-driven light sources, x-ray, free-electron lasers, spallation neutron sources, and intense proton drivers. Any beam degradation at low energy can be frozen into the beam longitudinal profile as the beam is accelerated, and all particles travel at the same velocity. It can therefore degrade high energy performance, for example, leading to serious consequences such as coherent synchrotron radiation or microbunching instability [14].

We present here the first comprehensive experimental study of soliton properties in electron beams. By generating controllable large-amplitude perturbations on long electron beams within a conducting pipe in the University of Maryland Electron Ring (UMER), we have observed consistent and reproducible KdV soliton wave train formation, over a wide range of parameters. Slow and fast waves emanating from the initial perturbation are observed to steepen sufficiently to balance wave dispersion, leading to a stable soliton wave train. We find that to generate solitons, the main conditions are a sufficiently high beam space charge intensity, a large perturbation amplitude (usually $>20\%$ of beam current), a long enough propagation distance (~ 10 times the perturbation length in the beam frame), and a relatively long perturbation pulse (scale length for density variation $\gg$ pipe radius).

Small initial perturbations are known to split into two space charge waves, a slow wave and a fast wave, going in opposite directions in the beam frame [15,16]. Larger perturbations are theoretically predicted to evolve into solitons, if the space charge in the beam is sufficiently strong [5,8]. The beam evolution can be shown to approximately evolve according to the KdV equation [6,8] known to describe soliton evolution:

$$\frac{\partial u}{\partial t} + \alpha u \frac{\partial u}{\partial z} + \beta \frac{\partial^3 u}{\partial z^3} = 0, \qquad \alpha, \beta \text{ constants}, \tag{1}$$

where $u(z, t)$ is the density or velocity perturbation amplitude, as a function of longitudinal distance z and propagation time t. The second term represents the nonlinear effect that steepens and narrows the perturbation until it is comparable to the pipe diameter, resulting in several subpulses. The third term is the dispersion that tends to widen the pulse. The soliton arises from the cancellation of these two terms. An analytical solution to the KdV equation shown above is the single-soliton solution

$$u(z, t) = \frac{3c}{\alpha} \operatorname{sech}^2\left[\frac{1}{2}\sqrt{\frac{c}{\beta}}(z - ct)\right], \tag{2}$$

where c is wave speed. The evolution of a known initial perturbation profile $u(z, t = 0)$ can be found by integrating the KdV equation over a time period τ to obtain $u(z, t = \tau)$. A numerical example is shown in Ref. [2] that illustrates a soliton train formation from a single initial pulse. We expect a similar perturbation evolution in experiments.

Under similar conditions as in the numerical example, we experimentally generated on UMER a scaled 11.42 m

circumference storage ring designed for exploring the physics of space charge over a wide range of intensities. The 10 keV electron beam is injected as a single long, rectangular bunch, with a duration of 100 ns. No longitudinal focusing is applied for the experiments presented here so the bunch ends expand freely within the ring and an ablation front decreases the length of the initial flattop bunch. By means of apertures immediately downstream from the anode, we can vary the peak beam current and rms emittance. The electron gun is a gridded Pierce-type gun with a thermionic dispenser cathode, made of a porous tungsten (W), coated with barium oxide (work function ~2.2 eV) and calcium aluminate. The gun can also generate beams by photoemission, driven by a Nd-YAG laser (1064 nm), with a FWHM pulse width about 5 ns, using two nonlinear crystals to triple the frequency (355 nm) such that the photon energy is sufficient to generate photoemission from the cathode. By operating the gun in the temperature-limited mode (650–850 °C), where the beam current can be easily modified by the cathode heater voltage, the additional electrons generated by the drive laser appear as a density perturbation superimposed on the long rectangular thermionic bunch. More details on the experimental setup and procedure can be found in Ref. [17]. For these experiments, the peak beam current varies over a range of 20–50 mA with an emittance that varies in the range of 1.5–3 μm (normalized).

The initial currents, with and without the perturbation, are measured using a fast current transformer (Bergoz) placed 64 cm from the cathode in the injection line. In the ring, the current is measured once per turn using a wall current monitor (WCM) located 7.67 m downstream from injection into the 11.52 m circumference ring.

Measurements with small initial perturbations confirm theoretical predictions and earlier experimental results [18], observing a slow and fast wave in the beam frame with identical sound speeds,

$$\mathrm{Cs} = \sqrt{\frac{qg\lambda_0}{4\pi\varepsilon_0\gamma_0^5 m}}. \quad (3)$$

In Eq. (3), q and m are the charge and mass of beam particles, g is the geometry factor [18], and λ_0 is the unperturbed beam line charge density. When the perturbation amplitude is large (say, >20% of beam current), the linear approximation no longer stands, and the particles on the crest travel faster than the ones on the trough, so that the wave will eventually steepen. Meanwhile, when the steepened wave-front width is comparable to the pipe radius, the wave becomes dispersive [5] and could balance the steepening. These two opposing phenomena—steepening and dispersion—are the mechanisms behind the generation of a stable, dispersion-less KdV-type soliton pulse.

Figure 1 shows the turn-by-turn plot of the beam current, measured with the WCM, for a typical experiment with a large-amplitude initial perturbation. The peak beam current is 22 mA, and the perturbation amplitude measured at the Bergoz coil is 5.5 mA above that (i.e., a 25% perturbation). We introduce the perturbation at the trailing edge of the beam so that there is the maximum distance for us to monitor the fast wave propagation on the beam, while the slow wave rolls off the edge. The fast wave steepens and develops into a wave train after a couple of turns. Starting near the fifth turn, as illustrated in Fig. 2, the subpulses of the train maintain their shapes, which is a basic property of solitons. The amplitude and width of each subpulse then remain constants within measurement error. Also, the subpulse width is measured to be about 1 ns, which is 6 cm long

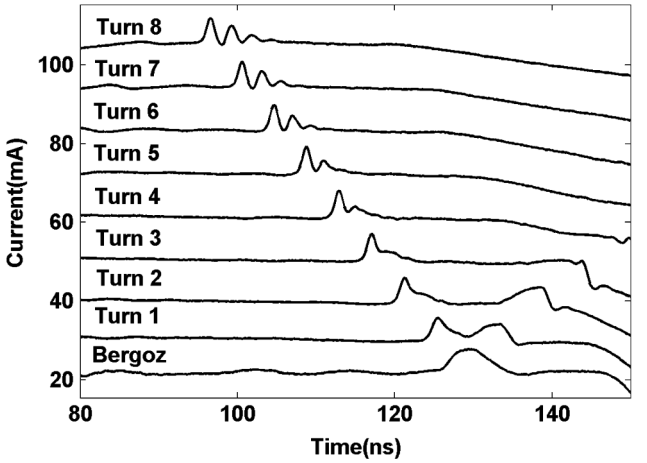

FIG. 1. Turn-by-turn plot of 22 mA beam with 25% perturbation propagation at Bergoz and RC10. As the turn increases, the initial pulse starts to develop into a soliton wave train. The perturbation is introduced near the tail of the beam to allow the fast wave to spend a longer time in the flattop portion of the beam. The beam currents are represented by positive values. For better comparison, the beam current is shifted upward by 12 mA on the plot after every turn.

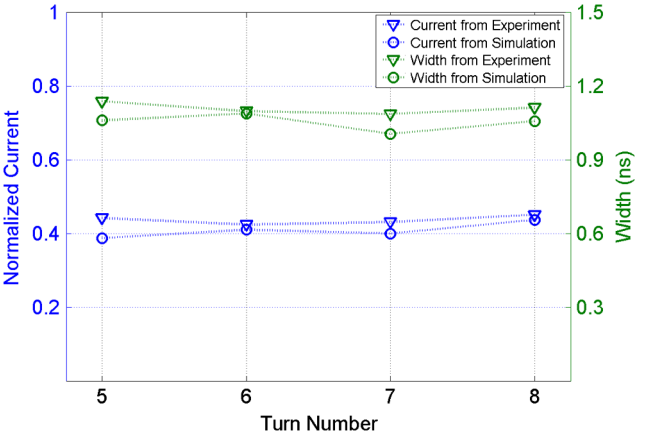

FIG. 2 (color online). Width and amplitude of the first subpulse at different turns in the ring (both experiment and simulation). The normalized current = perturbation current/unperturbed beam current.

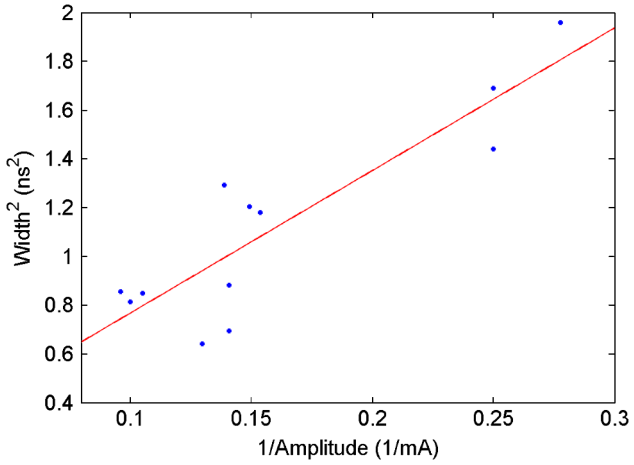

FIG. 3 (color online). Plot of soliton width^2 vs 1/amplitude, along with its linear fit, using the data points from the first and second subpulses in the wave train at the fifth, sixth, and seventh turns of 22 mA 25% perturbation experiment and 22 mA 50% perturbation experiment, respectively.

while the pipe diameter is comparably 5.08 cm, so that the dispersion effect is sufficient to balance the wave steepening. Because of the complex transverse dynamics we observe a ~10% loss in beam current at injection and a 5% loss per turn thereafter. The changing beam current results in a continually decreasing wave speed that may cause modification to the soliton amplitude and width.

To support the assertion that solitons are, in fact, what we observe, the KdV analytic model is used Eq. (1), According to the KdV soliton solution in Eq. (2), the width of the soliton (w) is inversely proportional to the square root of its amplitude (A) (Fig. 3); in other words, $w^2A =$ const. Another defining characteristic of the soliton is an amplitude dependence on the phase velocity of the soliton, increasing with amplitude growth (Fig. 4).

We performed additional experiments to confirm that the observed waves have another soliton characteristic: "They

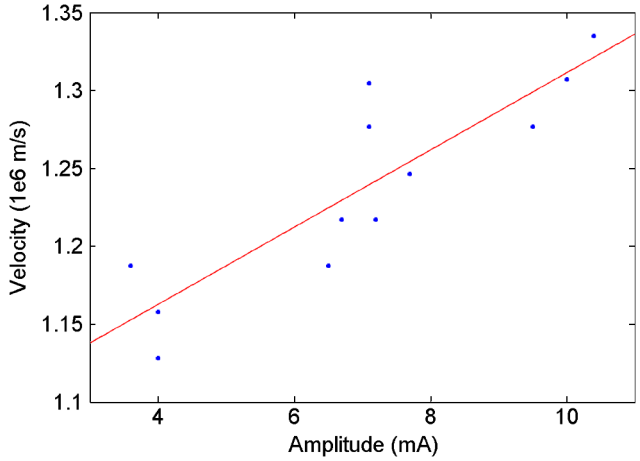

FIG. 4 (color online). Plot of soliton velocity vs amplitude, along with its linear fit, using the same data points with Fig. 3.

can interact with other solitons, and emerge from the collision unchanged, except for a phase shift" [19]. We use two lasers to generate two perturbations on both sides of the beam, and we let them propagate toward each other and then interact. We extend the beamwidth to 140 ns, to give the two perturbations enough time to propagate and steepen before they collide. As Fig. 5 illustrates, the two wave trains emerge completely unmodified by the collision. Comparison with an experiment with only one perturbation reveals little difference in the shape and amplitude of the subpulses after the collision.

To further understand the experiment, we simulated the evolution of the beam perturbation using the WARP particle-in-cell code [20] in an R-Z geometry. We input the initial beam density and velocity (assumed uniform) profiles at the cathode and extract the current profile (multiply density by velocity) turn by turn at the WCM, 7.67 m downstream. A smooth focusing approximation is assumed to represent the 36 alternating-gradient lattice each turn, with a focusing strength of $\kappa = 13.33\ \mathrm{m}^{-2}$. The beam is straightened, i.e., assumed to be propagating in a straight pipe. Previous experiment-simulation comparisons have shown excellent agreement between the experiment and the model [21]. The transverse distribution is assumed to be semi-Gaussian (uniform in space and Gaussian in velocity, with a uniform temperature). We assumed an initial beam radius of 9.5 mm with zero slope. The kinetic energy is 10 keV with a longitudinal thermal spread $\frac{\Delta p}{p} = 0.1\%$. We used 4 million macroparticles, a time step of 1 ns, 64 cells radially, and 2048 cells axially. The size of the simulation region is 0.0254 m in R, with a conducting boundary, and 11.52 m in z with periodic boundary conditions to reflect the periodicity of the ring. Numerical parameters have been thoroughly tested to reach convergence.

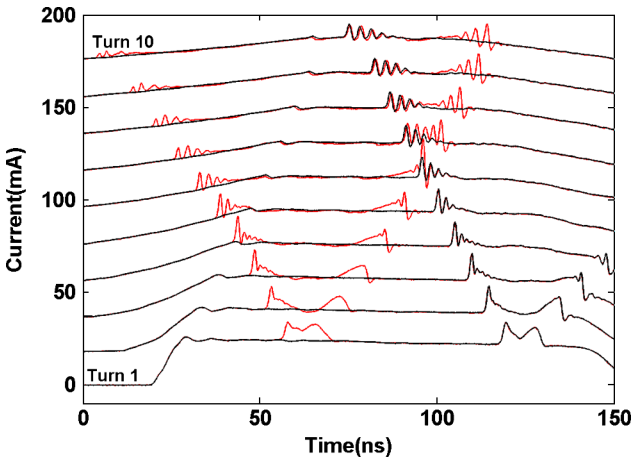

FIG. 5 (color online). Comparison of two-perturbation experiment and one-perturbation experiment (30 mA, 50%). The fast wave of the right perturbation interacts with the slow wave of the left perturbation (red; gray) and is compared with the fast wave propagation of the one perturbation experiment (black).

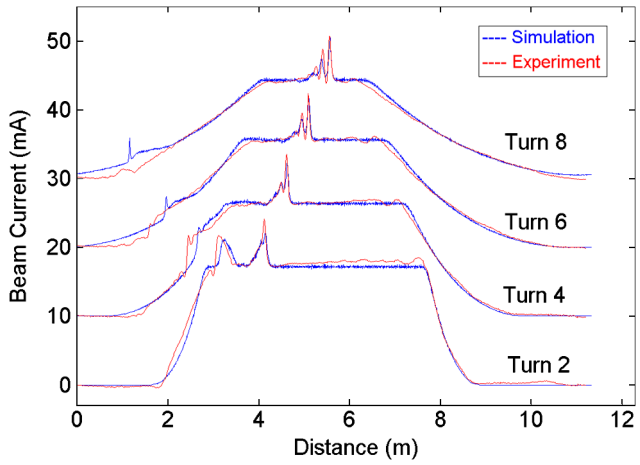

FIG. 6 (color online). Current profile comparison between experiment (red) and simulation (blue) at WCM for different turns. Reasonable agreement is achieved on the soliton wave train profile, current loss, sound speed, and beam edge erosion rate. Beam current is shifted upward by 10 mA every two turns for better comparison.

A typical comparison between simulation and experiment is shown in Fig. 6; using an adjusted initial condition at the cathode, reasonable agreement is achieved.

There are several complications that might affect the agreement between simulation and experiment. First, the beam loss can substantially modify the longitudinal dynamics. In the simulation, we assume a uniform beam loss along the bunch and a loss rate that is constant in time between the discrete measurements once per turn. The loss in the experiment may not be so uniform, especially right after the injection. Second, the initial current profile at the cathode is unknown. The first measurement is 64 cm downstream at the Bergoz. The perturbation widens by the time it reaches there. Also, the initial density modulation could lead to a velocity modulation at the Bergoz, and it further widens the current perturbation. In addition, we use uniform focusing in the simulation, approximating the varying beam radius in an alternating-gradient lattice with a constant radius that is the average of measured beam sizes at different chambers. Despite all those factors above, the overall agreement between simulation and experiment is quite good.

In conclusion, we report in this Letter the first experimental observation of soliton wave trains on an electron beam observed to result from deliberately introducing large-amplitude density perturbations. The results agree reasonably well with theory and simulation. We expect to refine our detailed understanding as ongoing efforts to optimize the UMER operation result in a reduction of beam losses.

The findings presented here are scalable to larger accelerators, provided the relative strengths of space charge to external forces are the same. We also plan future investigations of this phenomenon that study the possibility of soliton reflection at the beam end in the presence of induction focusing, the generation of solitons from initial velocity modulations (using the induction cell to modulate velocities), investigating the effects of wall impedance, and the effect of beam transverse distribution on the soliton characteristics.

We expect such a soliton-train modulated electron beam to potentially be used as a tunable, coherent radiation source. In addition, the shape preserving property of a soliton-type pulse could be a novel way to generate a femtosecond electron bunch using bunch compression with little degradation in the shape as in optical soliton lasers.

We thank R. Davidson, E. Startsev, H. Qin, I. Kaganovich, J. Harris, J. Bisognano, and S. Koscielniak for helpful discussions, and A. Friedman, D. Grote, and J.-L. Vay for their support of WARP. This work is supported by the U.S. Department of Energy Offices of High Energy Physics and Fusion Energy Sciences, and the Department of Defense Office of Naval Research and the Joint Technology Office.

*Present address: Accelerator Physics Center, Fermi National Laboratory, Batavia, Illinois 60510, USA.

[1] J. Scott Russell, *Report of the Fourteenth Meeting of the British Association for the Advancement of Science, York, September 1844* (Richard and John E Taylor, London, 1845), pp. 311–390, Plates XLVII-LVII.
[2] N. J. Zabusky and M. D. Kruskal, Phys. Rev. Lett. **15**, 240 (1965).
[3] H. Ikezi, R. J. Taylor, and D. R. Baker, Phys. Rev. Lett. **25**, 11 (1970).
[4] M. Reiser, *Theory and Design of Charged Particle Beams* (Wiley-VCH Inc., Weinheim, Germany, 2008), 2nd ed.
[5] J. Bisognano, I. Haber, L. Smith, and A. Sternlieb, IEEE Trans. Nucl. Sci. **28**, 2513 (1981).
[6] J. Bisognano, *High-Brightness Beams for Advanced Accelerator Application, Particles and Fields*, AIP Conf. Proc. Vol. 47 (AIP, New York, 1992), p. 42.
[7] H. Suk, J. G. Wang, and M. Reiser, Phys. Plasmas **3**, 669 (1996).
[8] R. Davidson, Phys. Rev. ST Accel. Beams **7**, 054402 (2004).
[9] R. Davidson, E. Startsev, and Hong Qin, in *Proceedings of PAC07, Albuquerque, New Mexico, 2007* (IEEE, Piscataway, NJ, 2007), p. 4291.
[10] H. Schamel, Phys. Rev. Lett. **79**, 2811 (1997).
[11] O. Boine-Frankenheim and I. Hofmann, Phys. Rev. ST Accel. Beams **3**, 104202 (2000).
[12] M. Blaskiewicz and J. Wei, Phys. Rev. ST Accel. Beams **7**, 044402 (2004).
[13] S. Koscielniak, S. Hancock, and M. Lindroos, Phys. Rev. ST Accel. Beams **4**, 044201 (2001).
[14] T. Shaftan and Z. Huang, Phys. Rev. ST Accel. Beams **7**, 080702 (2004).
[15] J. G. Wang, D. X. Wang, and M. Reiser, Phys. Rev. Lett. **71**, 1836 (1993).

[16] K. Tian, R. A. Kishek, I. Haber, M. Reiser, and P. G. O'Shea, Phys. Rev. ST Accel. Beams **13**, 034201 (2010).

[17] Y. Mo *et al.*, in *Proceedings of the IEEE Particle Accelerator Conference, New Orleans, LA, 2012* (IEEE, Piscataway, NJ, 2012), p. 1377.

[18] J. G. Wang, H. Suk, D. X. Wang, and M. Reiser, Phys. Rev. Lett. **72**, 2029 (1994).

[19] P. G. Drazin and R. S. Johnson, *Solitons: An Introduction* (Cambridge University Press, Cambridge, England, 1989), 2nd ed.

[20] D. P. Grote, A. Friedman, I. Haber, and S. Yu, Fusion Eng. Des. **32–33**, 193 (1996).

[21] T. Koeth *et al.*, in *Proceedings of the IEEE Particle Accelerator Conference, New York, NY, 2011* (IEEE, Piscataway, NJ, 2011), p. 22.